On the Performance of Four-Node Quadrilateral Element for Structural Topology Optimization

Carlos Millan-Paramo, João Elias Abdalla Filho, and Jair de Jesus Arrieta Baldovino

Abstract— The purpose of this work is to evaluate the performance of a four-node quadrilateral element for topology optimization of a two-dimensional linear elastic structure. The formulation of the element is developed within the framework of the strain gradient notation with the aim that the analyst can physically interpret its modeling capabilities and deficiencies. Therefore, parasitic shear commonly encountered in four-node quadrilateral elements is identified as caused by spurious terms which appear in the shear strain expansions. These spurious terms are simply removed to correct the element model. The results show that the correct model converges faster than the element with parasitic shear.

Index Terms— Topology optimization, strain gradient notation, parasitic shear, finite element method.

I. INTRODUCTION

TOPOLOGY optimization (TO) seeks to obtain the optimal material layout within a specific design space for a given set of loads, constraints and boundary conditions with the purpose of maximize the performance of the system. TO is a relatively new but rapidly expanding field of research, with interesting theoretical implications in mathematics, mechanics, physics, and computer science, but also important practical applications by the manufacturing industries (in particular, automotive and aerospace) and will likely have a significant role in micro and nanotechnologies [1].

In the last few decades, TO for continuous structures has been extensively explored. Several optimization methods, such as Homogenization Method [2], Evolutionary Structural Optimization (ESO) [3] and Solid Isotropic Material with Penalization (SIMP) [4] were developed.

In the homogenization method, it is assumed that the structural domain is completely occupied by a composite material. The material is inhomogeneous with an adjustable microstructure that switches between solid and void in the optimization process. Therefore, in order to shape a new material distribution in the domain, the material will be moved from one part of the structural domain to the other. This new distribution will lead to an optimal material distribution that provides the optimal design of a structure. This method produced promising results encouraging the investigation of new techniques and approaches in structural optimization and has been successfully applied in the optimization of linearly elastic structures [5]–[7]. The general advantages of the homogenization method are its precise theoretical basis and good convergence behavior. However, the use of traditional methods (deterministic methods) and mathematical programming make it difficult to reach the global optimum. Recently, homogenization approaches have fallen into disuse, giving way to the SIMP approach to TO.

With finite element analysis, the ESO method was initially proposed, gradually removing inefficient material until a desired optimal solution is reached. An extended version of this method is called the bidirectional ESO (BESO) method. BESO allows material to be added to the design domain [8], [9]. As design variables can be removed during the optimization process, tuning parameters must be optimized. ESO/BESO methods are heuristic methods that are used to find the best solution among the many solutions generated in the optimization process [10]. Recent applications of this method in the design of advanced structures and materials are summarized in the work of Xie [11]. According to Rozvany [1], the disadvantage of ESO is that it is completely heuristic, so there is no rigorous proof that the eliminations of elements provide an optimal solution. Furthermore, ESO generally requires a much larger number of iterations and can produce a totally non-optimal solution.

The SIMP method [12] is another widely used topology optimization method. In this method, the design domain is discretized into finite elements and a given amount of material is uniformly distributed in the design domain, minimizing or maximizing the objective function. The material density of each element is treated as the design variable. This can continuously vary from 0 (empty) to 1 (solid) for absence of material and presence of material. Meanwhile, the characteristics of the intermediate densities are artificially penalized in the objective function. The main benefit of employing the penalty function is that only expressions for element deformation and kinetic energies are needed for sensitivity analysis. In addition, any commercial finite element package can be used directly in TO problems. This method has inspired the development of new methodologies (e.g., [13]–[16]) and it is still used as a base method to develop new TO methodologies [17]–[22]. Despite the many applications of the method and its simplicity and versatility [23], a disadvantage of SIMP is that it is not possible to guarantee an optimal global solution for highly complex and non-convex problems [1]. Also, the

Carlos Millan-Paramo is a Professor at the Department of Civil Engineering, Universidad de Sucre, Sincelejo, Colombia, e-mail: carlos.millan@unisucre.edu.co
João Elias Abdalla Filho is a Professor at the Postgraduate Program in Civil Engineering (PPGEC), Federal University of Technology- Paraná, St. Dep. Heitor Alencar Furtado, 5000, Campus Curitiba, CEP: 81280-340, Ecoville, Paraná, Brazil, e-mail: joaofilho@utfpr.edu.br
Jair de Jesus Arrieta Baldovino is a Professor at the Department of Civil Engineering, Universidad de Cartagena, Cartagena de Indias 130015, Colombia, e-mail: jarrietab2@unicartagena.edu.co

number of iterations to converge to the optimum can be large. [24], [25].

Most TO problems are non-convex, that is, within the solution space there are several local minima, which leads to different optimal solutions for the same problem. To counteract this drawback, in this work, the finite element (four-node quadrilateral) used in the discretization of structural elements, is formulated using strain gradient notation (SGN), a physically interpretable notation, which has been developed by Dow [26]. In the following sections the TO problem is formulated, the four-node quadrilateral element is described in the SGN, and the problems and discussions are presented.

II. Problem Formulation

The objective of the optimization problem is to find the optimal material distribution, in terms of the minimization of the objective function, with a constraint on the total amount of material [15]. In this work, the modified SIMP methodology introduced by Andreassen [15] is used. The design domain is discretized by finite elements and each element is assigned a density x_e that determines its modulus of elasticity E_e:

$$E_e(x_e) = E_{min} + x_e^p(E_0 - E_{min}) \tag{1}$$

where E^0 is the stiffness of the material, E_{min} is a very small stiffness assigned to void regions in order to prevent the stiffness matrix from becoming singular, and p is a penalization factor (typically p=3) introduced to ensure black-and-white solutions [15].

The mathematical formulation of the optimization problem is as follows:

$$\text{minimize:} \quad c(x) = U^TKU = \sum_{e=1}^{N} E_e(x_e)u_e^Tk_0u_e \tag{2}$$

$$\text{subject to:} \quad \begin{cases} V(x)/V_0 = f_v \\ KU = F \\ 0 \leq x \leq 1 \end{cases}$$

where c is the compliance, U and F are the global displacement and force vectors, respectively, K is the global stiffness matrix, u_e is the element displacement vector, k_0 is the element stiffness matrix for an element with unit Young's modulus, x is the vector of design variables (i.e., the element densities), N is the number of elements used to discretize the design domain, $V(x)$ and V_0 are the material volume and design domain volume, respectively, and f_v is the prescribed volume fraction.

III. Four-Node Quadrilateral Element

SGN is a physically interpretable notation that explicitly relates displacements to kinematic quantities of the continuum [27]. Such kinematic quantities are rigid body motions, strains and their derivatives, and are generally referred to as strain gradients. The relationships between the displacement components and strain gradients are obtained through an algebraic procedure in which the physical contents of the coefficients of the approximation functions

are determined. The procedure is fully described, and the results are tabulated in Dow [26]. Other references related to SGN and its applications are [27]–[36].

Due to the physically interpretable character of the NSG, the finite element modeling characteristics are evident from the first steps of the formulation. This allows the identification of spurious terms that cause the artificial stiffening inherent in traditional formulations. NSG is described in this section through the four-node quadrilateral formulation for plane state analysis. The displacement field for this element is [26]:

$$u(x,y) = a_1 + a_2x + a_3y + a_4xy$$
$$v(x,y) = b_1 + b_2x + b_3y + b_4xy \tag{3}$$

The two zeroth-order terms, a_1 and b_1, can be evaluated immediately in terms of the displacements of the rigid body, $(u_{rb})_0$ and $(v_{rb})_0$. This is achieved by evaluating equations (3) at the element origin. All terms except the main constant terms are eliminated because they are functions of x and y. When this substitution is made and the displacements at the origin are recognized as the displacements of the rigid body, the principal constants of the displacement polynomials are [26]:

$$a_1 = (u_{rb})_0$$
$$b_1 = (v_{rb})_0 \tag{4}$$

First-order terms (linear) are evaluated in terms of rotation and the three components of deformation at the origin. Rotation around the z-axis is the rotation-displacement relation from the small displacement theory of elasticity [26]:

$$r_{rb} = \frac{1}{2}\left(\frac{\partial v}{\partial x} - \frac{\partial u}{\partial y}\right) \tag{5}$$

Similarly, the strain-displacement relations are [26]:

$$\varepsilon_x = \frac{\partial u}{\partial x}$$
$$\varepsilon_y = \frac{\partial v}{\partial y}$$
$$\gamma_{xy} = \frac{\partial u}{\partial y} + \frac{\partial v}{\partial x} \tag{6}$$

Evaluating Equations (5) and (6) at the origin results in [26]:

$$(r_{rb})_0 = \frac{1}{2}(b_2 - a_3)$$
$$(\varepsilon_x)_0 = a_2$$
$$(\varepsilon_y)_0 = b_3$$
$$(\gamma_{xy})_0 = a_3 + b_2 \tag{7}$$

These expressions are solved for the arbitrary coefficients to give [26]:

$$a_2 = (\varepsilon_x)_0$$
$$a_3 = \left(\frac{\gamma_{xy}}{2} - r_{rb}\right)_0$$
$$b_2 = \left(\frac{\gamma_{xy}}{2} + r_{rb}\right)_0 \tag{8}$$
$$b_3 = \left(\varepsilon_y\right)_0$$

Calculating the derivatives $\varepsilon_{x,y}$ and $\varepsilon_{y,x}$, called strain gradients:

$$a_4 = \left(\varepsilon_{x,y}\right)_0$$
$$b_4 = \left(\varepsilon_{y,x}\right)_0 \tag{9}$$

The approximate displacement representations for the four-node quadrilateral element are [26]:

$$u(x,y) = (u_{rb})_0 + (\varepsilon_x)_0 x + \left(\frac{\gamma_{xy}}{2} - r_{rb}\right)_0 y + (\varepsilon_{x,y})_0 xy$$
$$v(x,y) = (v_{rb})_0 + \left(\frac{\gamma_{xy}}{2} + r_{rb}\right)_0 x + (\varepsilon_y)_0 y + (\varepsilon_{y,x})_0 xy \tag{10}$$

When the displacement approximations for the four-node quadrilateral are substituted into the definitions of strain, the strain representations contained in this element are [26]:

$$\varepsilon_x = (\varepsilon_x)_0 + (\varepsilon_{x,y})_0 y$$
$$\varepsilon_y = (\varepsilon_y)_0 + (\varepsilon_{y,x})_0 x \tag{11}$$
$$\gamma_{xy} = (\gamma_{xy})_0 + (\varepsilon_{x,y})_0 x + (\varepsilon_{y,x})_0 y$$

The use of NSG makes it evident that the shear strain expression γ_{xy} for this element contains two erroneous flexure terms, $(\varepsilon_{x,y})_0$ and $(\varepsilon_{y,x})_0$. The effect of this error can be described as follows. When the strain energy is calculated, these two terms are carried over to the shear strain component, adding strain energy to the element, which makes the element excessively rigid [26]. This modeling error is known as parasitic shear [26].

Equation (11) can be written in matrix form as:

$$\{\varepsilon\} = [T]\{\varepsilon_{,}\}$$
$$\{\varepsilon\}^T = \{\varepsilon_x \quad \varepsilon_y \quad \gamma_{xy}\}$$
$$\{\varepsilon_{,}\}^T = \{(u_{rb})_0 \ (v_{rb})_0 \ (r_{rb})_0 \ (\varepsilon_x)_0 \ (\varepsilon_y)_0 \ (\gamma_{xy})_0 \ (\varepsilon_{x,y})_0 \ (\varepsilon_{y,x})_0\} \tag{12}$$
$$[T] = \begin{bmatrix} 0 & 0 & 0 & 1 & 0 & 0 & y & 0 \\ 0 & 0 & 0 & 0 & 1 & 0 & 0 & x \\ 0 & 0 & 0 & 0 & 0 & 1 & \underline{x} & \underline{y} \end{bmatrix}$$

These erroneous terms are contained in the shear strain component of Equation (12) by the x and y terms that are underlined. Parasitic shear can be removed from the element by removing these two erroneous terms [26].

The next step is to obtain a relationship between the nodal displacements and the strain gradient variables that governs the deformations of the element.

$$\{d\} = [\Phi]\{\varepsilon_{,}\}$$
$$\begin{Bmatrix} u_1 \\ v_1 \\ u_2 \\ v_2 \\ u_3 \\ v_3 \\ u_4 \\ v_4 \end{Bmatrix} = \begin{bmatrix} 1 & 0 & -y_1 & x_1 & 0 & y_1/2 & x_1 y_1 & 0 \\ 0 & 1 & x_1 & 0 & y_1 & x_1/2 & 0 & x_1 y_1 \\ 1 & 0 & -y_2 & x_2 & 0 & y_2/2 & x_2 y_2 & 0 \\ 0 & 1 & x_2 & 0 & y_2 & x_2/2 & 0 & x_2 y_2 \\ 1 & 0 & -y_3 & x_3 & 0 & y_3/2 & x_3 y_3 & 0 \\ 0 & 1 & x_3 & 0 & y_3 & x_3/2 & 0 & x_3 y_3 \\ 1 & 0 & -y_4 & x_4 & 0 & y_4/2 & x_4 y_4 & 0 \\ 0 & 1 & x_4 & 0 & y_4 & x_4/2 & 0 & x_4 y_4 \end{bmatrix} \begin{Bmatrix} (u_{rb})_0 \\ (v_{rb})_0 \\ (r_{rb})_0 \\ (\varepsilon_x)_0 \\ (\varepsilon_y)_0 \\ (\gamma_{xy})_0 \\ (\varepsilon_{x,y})_0 \\ (\varepsilon_{y,x})_0 \end{Bmatrix} \tag{13}$$

A discrete approximation of the strain energy written with strain gradient quantities as the independent variables, can be expressed as follow [26]:

$$U = \frac{1}{2}\{\varepsilon_{,}\}^T \left[\int_{\Omega} [T]^T [C][T] d\Omega\right] \{\varepsilon_{,}\}$$
$$U = \frac{1}{2}\{\varepsilon_{,}\}^T \overline{U}\{\varepsilon_{,}\} \tag{14}$$

The strain energy expression in terms of nodal displacements is:

$$U = \frac{1}{2}\{d\}^T [\Phi]^{-T} \overline{U} [\Phi]^{-1}\{d\} \tag{15}$$

The finite element stiffness matrix can be extracted from Equation (15) according to the principle of minimum potential energy as:

$$[K] = [\Phi]^{-T} \overline{U} [\Phi]^{-1} \tag{16}$$

IV. EXPERIMENTAL RESULTS AND DISCUSSIONS

In this section, the element whose formulation was described in Section III is applied in the solution of three TO benchmark problems. All experiments are run with two versions of the model, namely: a version containing the parasitic shear (PS) terms (with–PS) and a version after elimination of the parasitic shear terms(wout–PS) (corrected model).

For all examples, unitary modulus of elasticity was considered; Poisson's ratio $v=0.3$ and applied forces with unit values. The simulations are executed using an Intel Core i7-3630QM system 2.4 GHz with 8 GB RAM. The results, in terms of the topologies (Top), compliance (c), number of iterations (NI) and execution time (t) are presented in Tables I, II and III.

A. MBB beam

The first example analyzed is a MBB beam. The design domain and boundary conditions for this are shown in Figure 1. The load is applied vertically in the upper left corner and there are symmetrical boundary conditions along the left edge and the structure is supported horizontally in the lower right corner. The problem is analyzed using three different size meshes, namely 75x25, 150x50 and 300x100. In this problem, a prescribed volume fraction of 0.5 [15] is adopted, that is, a final volume of 50% of the initial volume.
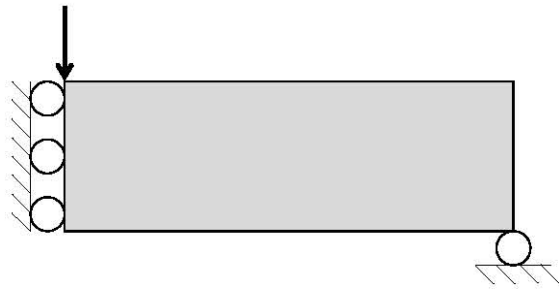
Fig. 1. MBB beam.

Table I shows the topologies, compliance values, number of iterations and execution time obtained with both elements. In general, it can be seen that the topologies and compliance values obtained do not show significant differences. The difference is in the speed of convergence.

For example, in the 150x50 mesh, the corrected model (wout–PS) reaches the optimal value in 169 NI (30.9 s) while the model with spurious terms (with–PS) needs 362 NI (67.3 s). The same goes for the 300x100 mesh refinement (813 s with–PS and 424.4 s wout–PS)

TABLE I
RESULTS COMPARISON FOR THE MBB BEAM

		with–PS	wout–PS
Mesh 75x25	Top		
	c	232.23	233.01
	NI	169	107
	t (s)	10.4	7.8
Mesh 150x50	Top		
	c	235.73	236.78
	NI	362	169
	t (s)	67.3	30.9
Mesh 300x100	Top		
	c	238.31	239.08
	NI	625	329
	t (s)	813.6	424.2

B. Cantilever beam

Figure 2 shows the design domain and boundary conditions for the cantilever beam. The beam was discretized in three types of mesh: 80x50, 160x100 and 320x200. The problem is optimized with a prescribed volume fraction of 0.4 [15]

Fig. 2. Cantilever beam.

Table II shows the strain energy values, number of iterations, execution time and topologies obtained. As in the previous example, the topologies and compliance values do not show major differences.

The results indicate that wout–PS model converges faster than with-PS model. For example, values associated with the 320x200 mesh show that wout–PS gets the optimal value in 497 NI (982.3 s) while with-PS needs 872 NI (1421.4 s).

TABLE II
RESULTS COMPARISON FOR THE CANTILEVER BEAM

		with–PS	wout–PS
Mesh 80x50	Top		
	c	63.07	63.44
	NI	202	165
	t (s)	17.8	14.7
Mesh 160x1000	Top		
	c	64.76	65.17
	NI	590	318
	t (s)	235.1	132.6
Mesh 320x200	Top		
	c	66.34	66.62
	NI	872	497
	t (s)	1421.4	982.3

C. Cantilever beam with two load cases

The last problem is the cantilever beam with two load cases (Figure 3). The problem is analyzed using three different size meshes, namely 50x50, 100x100 and 200x200. In this problem, a prescribed volume fraction of 0.4 [15] is adopted.
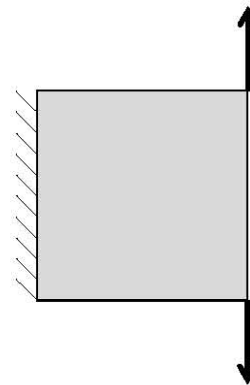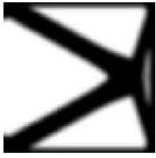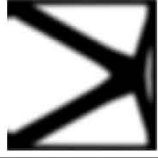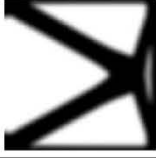

Fig. 3. Cantilever beam with two load cases.

Table III presents the values obtained for this problem. Numerical results indicate that the removal of spurious terms does not influence compliance values and topologies. However, it is worth mentioning that the removal of spurious terms leads this methodology (wout–PS) to converge more quickly. As can be seen, when the problem becomes more refined, this methodology shows its great convergence capacity (for 200x200 mesh, 109 NI for with–PS, 97 NI for wout–PS).

Finally, it can be concluded that the methodology that involves the corrected elements (wout-PS) is the most efficient. In the three problems analyzed in this work, this

methodology always obtained the optimal solution with less NI. In addition, its ability to solve problems with refined meshes is evidenced.

TABLE III

RESULTS COMPARISON FOR THE CANTILEVER BEAM WITH TWO LOAD CASES

		with–PS	wout–PS
Mesh 50x50	Top		
	c	68.17	68.98
	NI	71	47
	t (s)	5.2	3.8
Mesh 100x1000	Top		
	c	71.37	72.06
	NI	81	65
	t (s)	18.2	15.3
Mesh 200x200	Top		
	c	74.41	75.07
	NI	109	97
	t (s)	190.7	129.8

V. CONCLUSION

In this work, the use of the finite element (four-node quadrilateral) developed in the field of Strain Gradient Notation (SGN) was implemented for the first time to solve topological optimization problems.

Three benchmark problems were performed to show both the parasitic shear effects and that the corrected model provides good solutions. The results showed that the elimination of parasitic shear does not influence the topologies and optimal values of compliance. However, the difference is noticed in the convergence time. As the mesh was refined, the problems that were solved with corrected finite elements (wout-PS), converged to the optimal value in less time.

REFERENCES

[1] G. I. N. Rozvany, "A critical review of established methods of structural topology optimization," Struct. Multidiscip. Optim., vol. 37, no. 3, pp. 217–237, 2009.

[2] M. P. Bendsøe and N. Kikuchi, "Generating optimal topologies in structural design using a homogenization method," Comput. Methods Appl. Mech. Eng., vol. 71, no. 2, pp. 197–224, 1988.

[3] Y. M. Xie and G. P. Steven, "A simple evolutionary procedure for structural optimization," Comput. Struct., vol. 49, no. 5, pp. 885–896, 1993.

[4] M. P. Bendsøe, "Optimal shape design as a material distribution problem," Struct. Optim., vol. 1, no. 4, pp. 193–202, 1989.

[5] N. Olhoff, M. P. Bendsøe, and J. Rasmussen, "On CAD-integrated structural topology and design optimization," Comput. Methods Appl. Mech. Eng., vol. 89, no. 1–3, pp. 259–279, 1991.

[6] K. Suzuki and N. Kikuchi, "A homogenization method for shape and topology optimization," Comput. Methods Appl. Mech. Eng., vol. 93, no. 3, pp. 291–318, 1991.

[7] C. A. Soto and A. R. Díaz, "On the modelling of ribbed plates for shape optimization," Struct. Optim., vol. 6, no. 3, pp. 175–188, 1993.

[8] X. Y. Yang, Y. M. Xei, G. P. Steven, and O. M. Querin, "Bidirectional Evolutionary Method for Stiffness Optimization," AIAA J., vol. 37, no. 11, pp. 1483–1488, 1999.

[9] O. M. Querin, V. Young, G. P. Steven, and Y. M. Xie, "Computational efficiency and validation of bi-directional evolutionary structural optimisation," Comput. Methods Appl. Mech. Eng., vol. 189, no. 2, pp. 559–573, 2000.

[10] G. I. N. Rozvany and O. M. Querin, "Combining ESO with rigorous optimality criteria," Int. J. Veh. Des., vol. 28, no. 4, pp. 294–299, 2002.

[11] L. Xia, Q. Xia, X. Huang, and Y. M. Xie, "Bi-directional Evolutionary Structural Optimization on Advanced Structures and Materials: A Comprehensive Review," Arch. Comput. Methods Eng., vol. 25, no. 2, pp. 437–478, 2018.

[12] O. Sigmund, "A 99 line topology optimization code written in matlab," Struct. Multidiscip. Optim., vol. 21, no. 2, pp. 120–127, 2001.

[13] K. Suresh, "A 199-line Matlab code for Pareto-optimal tracing in topology optimization," Struct. Multidiscip. Optim., vol. 42, no. 5, pp. 665–679, 2010.

[14] V. J. Challis, "A discrete level-set topology optimization code written in Matlab," Struct. Multidiscip. Optim., vol. 41, no. 3, pp. 453–464, 2010.

[15] E. Andreassen, A. Clausen, M. Schevenels, B. S. Lazarov, and O. Sigmund, "Efficient topology optimization in MATLAB using 88 lines of code," Struct. Multidiscip. Optim., vol. 43, no. 1, pp. 1–16, 2011.

[16] F. Ferrari and O. Sigmund, "A new generation 99 line Matlab code for compliance topology optimization and its extension to 3D," Struct. Multidiscip. Optim., vol. 62, no. 4, pp. 2211–2228, 2020.

[17] W. Zuo and K. Saitou, "Multi-material topology optimization using ordered SIMP interpolation," Struct. Multidiscip. Optim., vol. 55, no. 2, pp. 477–491, 2017.

[18] O. Amir, N. Aage, and B. S. Lazarov, "On multigrid-CG for efficient topology optimization," Struct. Multidiscip. Optim., vol. 49, no. 5, pp. 815–829, 2014.

[19] H. Liu, Y. Wang, H. Zong, and M. Y. Wang, "Efficient structure topology optimization by using the multiscale finite element method," Struct. Multidiscip. Optim., vol. 58, no. 4, pp. 1411–1430, 2018.

[20] M. Bruggi and P. Duysinx, "Topology optimization for minimum weight with compliance and stress constraints," Struct. Multidiscip. Optim., vol. 46, no. 3, pp. 369–384, 2012.

[21] C. Talischi, G. H. Paulino, A. Pereira, and I. F. M. Menezes, "PolyTop: a Matlab implementation of a general topology optimization framework using unstructured polygonal finite element meshes," Struct. Multidiscip. Optim., vol. 45, no. 3, pp. 329–357, 2012.

[22] R. Ansola Loyola, O. M. Querin, A. Garaigordobil Jiménez, and C. Alonso Gordoa, "A sequential element rejection and admission (SERA) topology optimization code written in Matlab," Struct. Multidiscip. Optim., vol. 58, no. 3, pp. 1297–1310, 2018.

[23] S. Zargham, T. A. Ward, R. Ramli, and I. A. Badruddin, "Topology optimization: a review for structural designs under vibration problems," Struct. Multidiscip. Optim., vol. 53, no. 6, pp. 1157–1177, 2016.

[24] X. Huang and Y. M. Xie, "Evolutionary topology optimization of continuum structures with an additional displacement constraint," Struct. Multidiscip. Optim., vol. 40, no. 1–6, pp. 409–416, 2010.

[25] O. Sigmund and K. Maute, "Topology optimization approaches," Struct. Multidiscip. Optim., vol. 48, no. 6, pp. 1031–1055, 2013.

[26] J. O. Dow, A Unified Approach to the Finite Element Method and Error Analysis Procedures. Elsevier, 1999.

[27] J. E. Abdalla Filho, I. M. Belo, and J. O. Dow, "On a Four-Node Quadrilateral Plate for Laminated Composites," Lat. Am. J. Solids Struct., vol. 14, no. 12, pp. 2177–2197, 2017.

[28] J. O. Dow, T. H. Ho, and H. D. Cabiness, "Generalized Finite Element Evaluation Procedure," J. Struct. Eng., vol. 111, no. 2, pp. 435–452, 1985.

[29] J. O. Dow and D. E. Byrd, "The identification and elimination of artificial stiffening errors in finite elements," Int. J. Numer. Methods Eng., vol. 26, no. 3, pp. 743–762, 1988.

[30] J. O. Dow and D. E. Byrd, "Error estimation procedure for plate bending elements," AIAA J., vol. 28, no. 4, pp. 685–693, 1990.

[31] J. O. Dow and J. E. Abdalla, "Qualitative errors in laminated composite plate models," Int. J. Numer. Methods Eng., vol. 37, no. 7, pp. 1215–1230, 1994.

[32] J. E. Abdalla Filho and J. O. Dow, "An error analysis approach for laminated composite plate finite element models," Comput. Struct., vol. 52, no. 4, pp. 611–616, 1994.

[33] J. E. Abdalla Filho, F. A. Fagundes, and R. D. Machado, "Identification and elimination of parasitic shear in a laminated composite beam finite element," Adv. Eng. Softw., vol. 37, no. 8, pp. 522–532, 2006.

[34] J. E. Abdalla Filho, I. M. Belo, and M. S. Pereira, "A laminated composite plate finite element a-priori corrected for locking," Struct. Eng. Mech., vol. 28, no. 5, pp. 603–633, 2008.

[35] J. E. Abdalla Filho, I. M. Belo, and J. O. Dow, "A serendipity plate element free of modeling deficiencies for the analysis of laminated composites," Compos. Struct., vol. 154, pp. 150–171, 2016.

[36] J. E. Abdalla Filho, J. O. Dow, and I. M. Belo, "Modeling Deficiencies in the Eight-Node Mindlin Plate Finite Element Physically Explained," J. Eng. Mech., vol. 146, no. 2, p. 04019131, 2020.